Nanotechnology Perceptions
ISSN 1660-6795
www.nano-*ntp.com*

Influence Of Surface Topography On Osteoblast Cell Adhesion On Polymeric Biomaterials: A Systematic Review

Geetha Lakshmi Munuswamy[1], Narasimha Raghavan. R[2*]

[1].Geetha Lakshmi Munuswamy, Senior Assistant Professor,Department of Orthodontics and dentofacial Orthopaedics, TamilNadu Government Dental College and Hospital, Chennai. University affliated :The TN Dr.MGR Medical University, Guindy, Chennai
[2]. Narasimha Raghavan R, Director, RNR Research Services, Chennai 600100, director@rnrresearch.co.in*
**-Corresponding Author*

Background: Surface topography is known to affect osteoblastic adhesion; however, consolidated evidence regarding how polymeric surface topography affects adhesion is lacking in the literature.
Aims: To identify studies that investigate the effect of polymeric biomaterials' surface topography on osteoblast adhesion so that a descriptive summary of topographical features that enhance or impede osteoblast adhesion may be inferred.
Methods: Studies describing osteoblasts' adhesion to the surface topography of polymeric biomaterials were collected from PubMed, Scopus, ProQuest, EBSCO, EuropePMC, and IEEE Xplore. Studies describing other materials such as metals, ceramics or composites were excluded. Electrospun materials, nonfouling structures, nanoparticle-based materials and studies not describing cell adhesion were excluded. The review followed PRISMA 2020 guidelines.
Results: The search resulted in 27 articles for final inclusion in the review. Polymers described were PLLA, PCL, PLGA, Polystyrene and PMMA. Nano and microscale modifications were analysed in these studies, where nanoscale modification affected the cell adhesion number, while microscale modifications affected the cell shape and alignment.
Conclusion: Nanotopography (10–100 nm) with moderate microscale roughness (0.1 to 10 microns) may be the recommended topography for cell adhesion, based on studies included.

Keywords: Osteoblast adhesion; nanostructured polymer surfaces; microtopography; biomaterial surface engineering; hierarchical roughness; cell–substrate interactions.

Introduction

The surface of the material is the interface through which cells recognise a material, and the critical well-orchestrated sequence of events that happen from the moment of placement of the material into the physiological system influences the future clinical life of the placed implant.(1) Due to the significant role of material surface in biomaterials science, it has attracted the major attention of investigators regarding its design and customisation. When it comes to implants placed in bone, the concept gains greater importance due to the unique properties and requirements of osteoblasts that influence the longevity of clinical service of the implant.(2) Modification of surface topography has been seen as a successful method in

encouraging osteoblast adhesion and sometimes discouraging other types of cells from attachment such as fibroblasts and bacterial cells. (3) (4) (5)
Polymeric biomaterials are being increasingly used in current-day bone-related clinical needs for both resorbable and non-resorbable applications. Major advantages of polymers for non-resorbable applications include High Mechanical Strength and Stability, Reduced Stress Shielding, Biostability and Long-Term Reliability, Resistance to Corrosion and Fatigue, Superior Wear Resistance and Excellent Processability.(6) In case of nonresorbable applications, the advantages include Biocompatibility, Tunable Mechanical Properties, 3D Structural Versatility and Fabrication, Surface Bioactivity and Osteogenesis, Drug Delivery Potential, Lightweight and Cost-Effectiveness.(7)
The surface topography to biocompatibility relation has been well investigated with regard to titanium.(8) However, due to the rising use of polymeric biomaterials, there is a need to consolidate the existing evidence on the relation of the topography of polymers with osteoblast adhesion. In this connection, there is a specific lacuna in relevance to topography introduced by various techniques towards osteoblast cell response. While a large amount of literature is available that reports cell adhesion to polymeric materials, the specific consolidation is still not clearly seen in the literature.
This systematic review aims to identify studies that investigate the effect of polymeric biomaterials' surface topography on osteoblast adhesion so that a descriptive summary of topographical features that enhance or impede osteoblast adhesion may be inferred.

Methodology

Objectives
The aim of this systematic review is to synthesise and analyse the methodologies used in surface modification and measurement of cell adhesion and to provide a descriptive summary of topographical features that enhance or impede osteoblast adhesion. The review follows PRISMA 2020 reporting guidelines.

Review Question
The review question of the current systematic review is "What is the impact of surface topography on osteoblast adhesion to polymeric biomaterial surfaces?"

PICO Framework
The PICO framework is shown in Table 1 below.

Table. 1. PICO Framework

Component	Definition
Population (P)	Osteoblasts (primary cells or cell lines)
Intervention/Exposure (I)	Surface topography features (micro, nano, hierarchical) of polymeric biomaterials

Component	Definition
Comparator (C)	Smooth/non-patterned polymer surfaces or different topographies
Outcome (O)	Cell adhesion (quantitative measurements e.g., cell count, focal adhesion markers, adhesion strength)

Eligibility Criteria

Inclusion
Original research articles that report in vitro analysis of osteoblast adhesion on polymeric biomaterials with defined surface topographies and studies reporting cell adhesion (cell count, percentage adhesion, focal adhesion proteins). No restriction was placed on the date of publication.

Exclusion
The following types of articles were excluded:
- Reviews, editorials, conference abstracts without full data,
- Materials with non-polymeric components, such as Ceramics, Metals and Composites – exhibit fundamentally different surface energy, stiffness and protein adsorption. In this way, studies reporting chitosan were excluded to remove the confounding from intrinsically bioactive materials.
- Nanofibers and nanoparticles, since they bring in dimensional and surface area variables that deviate from planar topology-based research questions
- Studies reporting coatings and nonfouling studies were excluded, as they mask the role of surface topography.
- Studies that report regenerative materials and their resorption – to exclude confounding from time-related changes in topography
- Studies that report on stem cells and other non-osteoblastic cells
- Studies reporting chemical modifications and plasma-based modification – to focus on topography rather than chemistry.
- Studies that describe a technique for evaluation rather than evaluating the material
- Reports on gradient topographies/libraries and chemical composition-related outcomes – they report relative rather than absolute adhesion metrics.
- Studies not measuring cell adhesion (e.g., only proliferation without adhesion data).
- In vivo studies (unless they include quantification of initial osteoblast adhesion in vitro).

Search Strategies
Key Concepts of the search strategy were as follows:
1. **Osteoblasts:** osteoblast, osteogenic cells, MC3T3, MG-63, Saos-2
2. **Topography:** surface topography, microstructure, nanostructure, surface pattern, roughness, texture

3. **Polymeric Biomaterials:** polymers, biodegradable polymers, PLA, PLGA, PCL, PEG, polyurethane. In order not to miss any possible information on cell adhesion, chitosan was also included in the search, but later eliminated.
4. **Cell Adhesion:** adhesion, cell attachment, focal adhesion, adhesion strength

Specific strategies are shown below in Table 2.

Table 2. Search Strategies

PubMed	("osteoblast*" OR "osteogenic cell*" OR MC3T3 OR MG-63 OR Saos-2) AND ("surface topograph*" OR "surface roughness" OR microtopography OR nanotopography OR "surface pattern*" OR texture*) AND ("polymer*" OR PLA OR PLGA OR PCL OR chitosan OR PEG OR polyurethane) AND ("cell adhesion" OR "cell attachment" OR "focal adhesion" OR "adhesion strength")
Scopus	(TITLE-ABS-KEY ((osteoblast* OR "osteogenic cell*" OR MC3T3 OR MG-63 OR Saos-2)) AND TITLE-ABS-KEY (("surface topograph*" OR "surface roughness" OR microtopography OR nanotopography OR "surface pattern*")) AND TITLE-ABS-KEY ((polymer* OR PLA OR PLGA OR PCL OR chitosan OR PEG OR polyurethane)) AND TITLE-ABS-KEY (("cell adhesion" OR "cell attachment" OR "adhesion")) AND LANGUAGE (English)) AND (LIMIT-TO (SUBJAREA , "DENT") OR LIMIT-TO (SUBJAREA , "MEDI") OR LIMIT-TO (SUBJAREA , "CHEM") OR LIMIT-TO (SUBJAREA , "BIOC") OR LIMIT-TO (SUBJAREA , "MATE") OR LIMIT-TO (SUBJAREA , "ENGI"))
Proquest	TI,AB(osteoblast* OR "osteogenic cell*" OR MC3T3 OR "MG-63" OR "Saos-2") AND TI,AB(("surface topography" OR microtopograph* OR nanotopograph* OR "surface roughness" OR "surface pattern*" OR "microstructured surface" OR "nanostructured surface")) AND TI,AB(("polymeric biomaterial*" OR "polymer scaffold*" OR "polymer surface*" OR PLA OR PLGA OR PCL OR chitosan OR polyurethane OR PEG)) AND TI,AB(("cell adhesion" OR "cell attachment" OR "initial adhesion" OR "focal adhesion" OR vinculin OR integrin)) NOT TI,AB(proliferation OR differentiation OR mineralization)
EBSCO	(MH "Osteoblasts+" OR osteoblast* OR "osteogenic cell*") AND ("surface topograph*" OR "surface roughness" OR microtopography OR nanotopography OR "surface pattern*") AND (polymer* OR PLA OR

EuropePMC	PLGA OR PCL OR chitosan OR PEG OR polyurethane) AND ("cell adhesion" OR "cell attachment") (TITLE:osteoblast* OR ABSTRACT:osteoblast* OR TITLE:"osteogenic cell*" OR ABSTRACT:"osteogenic cell*" OR TITLE:MC3T3 OR ABSTRACT:MC3T3 OR TITLE:"MG-63" OR ABSTRACT:"MG-63") AND (TITLE:"surface topograph*" OR ABSTRACT:"surface topograph*" OR TITLE:microtopograph* OR ABSTRACT:microtopograph* OR TITLE:nanotopograph* OR ABSTRACT:nanotopograph* OR TITLE:"surface roughness" OR ABSTRACT:"surface roughness") AND (TITLE:"polymeric biomaterial*" OR ABSTRACT:"polymeric biomaterial*" OR TITLE:"polymer scaffold*" OR ABSTRACT:"polymer scaffold*" OR TITLE:PLA OR ABSTRACT:PLA OR TITLE:PLGA OR ABSTRACT:PLGA OR TITLE:PCL OR ABSTRACT:PCL) AND (TITLE:"cell adhesion" OR ABSTRACT:"cell adhesion" OR TITLE:"cell attachment" OR ABSTRACT:"cell attachment" OR ABSTRACT:"focal adhesion") NOT ABSTRACT:(proliferation OR differentiation OR mineralization) AND SRC:MED
IEEEExplore	("All Metadata":Osteoblast) AND ("All Metadata":adhesion) AND ("All Metadata":surface topography) AND ("All Metadata":Polymer)

Screening and Selection Process

The results were deduplicated and screened using title/abstract against eligibility criteria. Subsequently, full-text retrieval and screening were done. The flow of review is shown in the PRISMA flow diagram (Fig. 1)

Data Extraction

Data extraction was done to obtain the following information: Authors, Year, Material type, Topography type, Topography parameters, Surface modification process, Cell lines, Adhesion measurement and Outcome results. Narrative synthesis was performed.

Quality Assessment

Since a standardised RoB tool is not available, a modified RoB tool from CONSORT and ARRIVE was used. Risk of Bias Domains Used were as follows: D1 - Clear study objective and design, D2 - Adequate control surface (flat or baseline), D3 - Surface topography quantified and characterised, D4-Fabrication method reproducible and described, D5-Cell model appropriately described, D6-Adhesion measurement method valid and quantitative, D7-Statistical analysis and replicates reported. Judgments given were L = Low risk, M = Moderate risk, H = High risk, and U = Unclear risk.

RESULTS

Figure 1. PRISMA Flow chart (9)

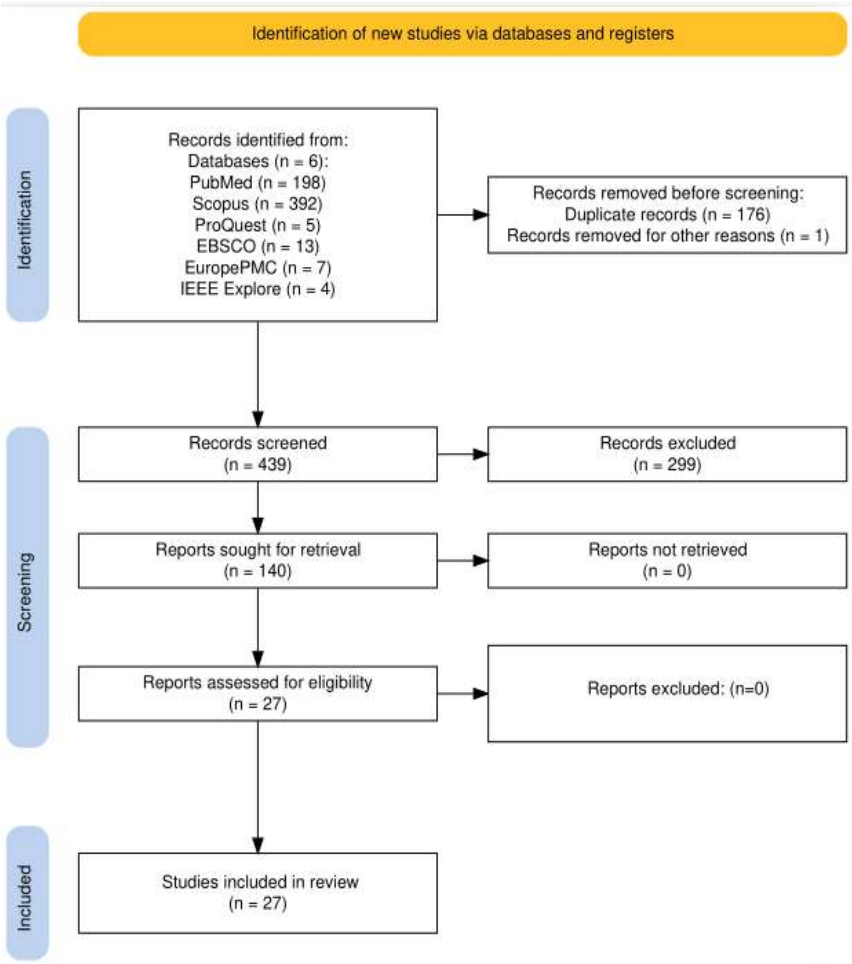

Table 1. Data Extraction

Authors (1st author et al.)	Year	Material type	Topography type	Topography parameters	Surface modification process	Cell model	Adhesion measurement	Outcome results
Ajami-Henriquez et al.(10)	2008	Poly(L-lactide) / poly(ε-caprolactone) blends and PLLA-b-PCL diblock copolymer	long range ordered domains (of the order of 2-3 mum)	Rq=4.57, Ra=3.63,	Nil	Rat calvarial osteoblasts	MTT	Satisfactory cell adhesion
Allan et al. (11)	2018	Polycprolactone	NSQ50 disordered	120 nm diameter, 100 nm deep pits,	electron-beam	SaOS-2 osteoblas	imaging	increased adhesion formation

			nanotopography		lithography	t-like cell line		& cytoskeletal organization
Barata et al.(12)	2017	Polylactic acid (PLA)	High-resolution micropatterns	between 500 nm and 15 µm	Direct laser lithography	MG63	cell morphometry	Cell behavior depending on microfeature design
Biggs et al.(13)	2009	Polystyrene	Multiple nanoscale topographies: nanopits (nanotopography with controlled disorder), nanocraters, nanoislands, nanogrooves.	Nanopits: near-square pits 120 nm diameter, 100 nm deep, ~300 nm spacing, ± disorder	Electron-beam lithography and polymer demixing to generate nanopits, nanocraters and nanoislands; nanogrooves by additional patterning.	Human osteoblasts (HOBs)	Immunocytochemistry, SEM and morphometry	Nanopit topographies inhibited large adhesion complexes in HOBs topographies reduced adhesion but upregulated osteospecific pathways.
Cha et al.(14)	2013	Polystyrene	Nanopillar and nanopore arrays (ordered nanotopographies).	Nanopillars and nanopores replicated from metal nanostamps; ~200nm diameter, ~500nm in depth.	Hot embossing	MC3T3-E1 osteoblast-like cells.	SEM	Nanoengineered surfaces significantly altered MC3T3-E1 morphology and attachment; nanopore arrays (NPS-Po) more effective than nanopillar

								s (NPS-Pi).
Dalby et al. (15)	2006	PMMA	Random nanoscale pits (nanotopography)	10 nm pits, c.ncbi.nlm.nih	Colloidal lithography and embossing	Osteoprogenitors (OPGs; human osteoprogenitor cells).	Imaging (Fluorescent)	Promoted adhesion
DeSantis et al. (16)	2026	PEKK	Microporous surface	Micron scale pores	Printing	Mouse MC3t3-E1	Imaging	Porous PEKK improved in vitro osteoblastic performance compared to PEEK.
Duan et al. (17)	2013	Poly(glycine ethyl ester-co-alanine ethyl ester) phosphazene (PGAP) vs PLGA reference	Honeycomb-patterned microporous surface topography	3-6 nm height = 12.03 μm, depth = 32.87 μm, Width of 28.7 μm. The surface roughness = 0.14 to 0.8 μm.	Chemical	MC3T3-E1	Cell counting kit	Honeycomb-patterned PGAP enhanced cell adhesion
Filipov et al. (18)	2022	Porous poly(ε-caprolactone) scaffolds	Ultra-short laser-textured porous surface patterns		Ultra-short pulsed laser texturing	MG63	Cell adhesion	Laser-textured porous PCL increased bone cell adhesion
Han et al.(19)	2022	Polycaprolactone (PCL) porous scaffolds	Porous surface	Sa 56.42 μm (Ed1, roughest) to 31.02 μm (Ed3, smoothest); pores 3-11 mm² area, porosity 45%	Selective laser sintering (SLS); energy densities Ed1=0.089, Ed2=0.178 (variants), Ed3=0.267	MC3T3-E1 mouse osteoblast precursors	Live/dead staining (Calcein-AM/PI)	Rougher surfaces had higher cell adhesion and flattened/spread morphology; smoother surface had sparse

					J/mm³ via laser power 2-6W, scan speed 750-2250 mm/s			round cells
Krysza k et al.(20)	2022	PLLA surfaces	Femtosecond laser-induced patterns	10-50 microns, Sa < 3.95; Sz <18.65	Femtose cond laser function alization	Osteobla sts	Neutral red assay and SEM	Tailored properties increased osteoblast adhesion
Lee et al. (21)	2004	Polycarbonate membranes	Micropore arrays	Different micropore sizes – 0.2 – 8 microns	Membra ne fabricati on with varying pore sizes	MG63 osteoblas t-like	Imaging and SEM	Cells spread better on smaller pore sizes (0.2-1 microns), appeared round on larger pores
Lenher t et al.(22)	2005	Grooved polystyrene	Grooved patterns	spaced grooves of different depths (50 and 150 nm) with a periodicity of 500 nm	Langmui r-Blodgett lithograp hy	Osteobla sts	Imaging	Osteoblas ts aligned/el ongated/ migrated on grooves
Li et al.(23)	2016	Poly(L-lactide) (PLLA)	Crystallization topography	sherulite surfaces	Crystalli zation control	MC3T3-E1	Imaging	PLLA cryst topograph y provides contact guidance to MC3T3-E1 cells adhesion
Lim et al.(24) (bioma c)	2005	Poly(L-lactic acid)/polystyren e (PLLA/PS) demixed thin films	Nanotopograp hy from phase demixing	island-dominant morphologies having nanoscale depth or	Polymer demixin g thin films	Osteobla sts	Adhesion affected by nano/wettab ility/chemist ry	Nanotextu red substrata stimulated osteoblast ic cell adhesion

				height (3-29 nm)				to a greater degree than did flat PLLA Cells on surfaces with 11nm high nanoislands displayed well-developed lamellipodia.
Lim et al.(25) (RSI)	2005	Polymer-demixed nanotopographic interfaces	Nanotopography from demixing	Island topography of 10-100 nm	Polymer demixing	Human foetal osteoblasts	Cell counting, Imaging and morphometry	
Lin et al.(26)	2023	Polylactic acid (PLA) implants	Surface microtopography	The ridge width of bulges ranged from 1.64 ± 0.16 µm to 82.52 ± 14.38 µm and the valley depth ranged from 0.49 ± 0.07 µm to 37.35 ± 6.78 µm	Microtopo construction	Osteoblasts	Imaging	Microtopography enhanced adhesion of cells
Maclaine et al.(27)	2012	Polycaprolactone (PCL)	Disordered nanotopography (14 nm and 18 nm features); planar control	Disordered pattern 14 nm and 18 nm features; roughness ~0.93 nm	Block copolymer phase separation; embossed onto PCL	Human osteoblasts	Imaging	Smaller feature nanopatterns improved adhesion Cell number decrease with increase in roughness ; 50 microns gap was the most
Melčová et al. (28)	2024	3D printed poly(3-hydroxybutyrate)/polylactide (PHB/PLA)	Surface roughness from printing	Upt0 150 microns grid	3D printing	Saos-2 osteosarcoma cells		

								favoured by cells
Riehle et al.(29)	2003	Polystyrene	Random nanometric features	45-100nm	Polymer phase separation	Rat calvaria bone cells ncbi.nlm.nih	Imaging	Nanofeatures increased adhesion
Smith et al.(30)	2007	PLGA scaffolds	Nanostructured (etch pits)	Nano-roughness from etching by NaOH	NaOH etching	Osteoblasts	Cell counting	Nanotopography increases osteoblast adhesion
Sun et al.(31)	2010	Polystyrene (PS), polymethylmethacrylate (PMMA), dimethacrylate (DMA)	Gradient nanogratings (line-and-space)	Height gradient 0-350 nm; two pitches – 420nm and 800nm; ridge/trough profile variations	Nanoimprint lithography (NIL) + annealing (PS/PMMA); photoimprint (DMA)	MC3T3-E1	Focal adhesions and imaging c.ncbi.nlm.nih	Cells oriented randomly at pattern heights less than 30 nm and aligned parallel to the grating direction at higher heights,
Wan et al.(32)	2005	Poly(L-lactide) (PLLA)	Micro- and nano-scale topography	0.45 micron dia for samll pits, 2.2 microns for large pits, space between them was ~1micron	Surface structuring (etching/ patterning)	OCT-1 osteoblast-like cells	SEM and cell counting	Micro/nano topography modulated OCT-1 adhesion/ proliferation
Wang et al. (33)	2000	Biodegradable polyesterurethane membranes	Variable porous surface morphologies	Varying phase morphologies	Membrane casting/phase inversion	Rat calvarial osteoblasts	Imaging	Rough surface enhanced osteoblast adhesion
Wang et al. (34)	2012	Poly(propylene fumarate)/poly(ε-caprolactone) (PPF/PCL) blends	Banded spherulitic morphology	Banded spherulites with concentric alternating succession of ridges and	Blend crystallization	MC3T3-E1 preosteoblasts	Cell interaction	More cells attached on the rougher surfaces than flat

				valleys – 35 to 350nm				ones. Cell nuclei were preferentially located close to the valleys. Nano-structures increased the preosteoblast adhesion
Yeon et al.(35)	2012	Block copolymer-surfactant nanostructured polymers	Nano-structured surfaces	Self-assembled nano-domains – 100nm	Block copolymer + surfactant complexation	Preosteoblasts	Imaging	
Yuanzheng et al. (36)	2026	3D-printed PLLA scaffolds	Etched nanotopography	~85 nm	3D printing & N-methyl-2-pyrrolidone etching	MC3T3-E1	Bone repairability	Etching enhanced bone cell adhesion

Table 2. Risk of Bias

Authors (1st author et al.)	**D1**	**D2**	**D3**	**D4**	**D5**	**D6**	**D7**	**Overall RoB**
Ajami-Henriquez et al.(10)	L	L	M	M	L	M	U	**Moderate**
Allan et al. (11)	L	L	L	L	L	L	L	**Low**
Barata et al.(12)	L	L	L	L	L	M	L	**Low**
Biggs et al.(13)	L	L	L	L	L	L	L	**Low**
Cha et al.(14)	L	L	L	L	L	M	M	**Moderate**
Dalby et al. (15)	L	L	L	L	L	M	U	**Moderate**
DeSantis et al. (16)	L	L	M	M	L	M	U	**Moderate**
Duan et al. (17)	L	L	M	M	L	M	M	**Moderate**

Filipov et al. (18)	L	L	L	L	L	L	L	**Low**
Han et al.(19)	L	L	L	L	L	L	L	**Low**
Kryszak et al.(20)	L	L	L	L	M	M	M	**Moderate**
Lee et al. (21)	L	L	L	L	L	M	U	**Moderate**
Lenhert et al.(22)	L	L	L	L	M	M	U	**Moderate**
Li et al.(23)	L	L	M	M	L	M	M	**Moderate**
Lim et al.(24) (biomac)	L	L	L	L	L	L	L	**Low**
Lim et al.(25) (RSI)	L	L	L	L	L	L	L	**Low**
Lin et al.(26)	L	L	L	M	M	M	M	**Moderate**
Maclaine et al.(27)	L	L	L	L	L	M	M	**Moderate**
Melčová et al. (28)	L	L	L	L	L	M	M	**Moderate**
Riehle et al.(29)	L	L	L	L	M	M	U	**Moderate**
Smith et al.(30)	L	L	M	M	L	L	M	**Moderate**
Sun et al.(31)	L	L	L	L	L	L	L	**Low**
Wan et al.(32)	L	L	M	M	M	M	U	**Moderate**
Wang et al. (33)	L	L	M	M	L	M	U	**Moderate**
Wang et al. (34)	L	L	L	L	L	M	M	**Moderate**
Yeon et al.(35)	L	L	M	M	L	M	M	**Moderate**
Yuanzheng et al. (36)	L	L	M	M	L	M	U	**Moderate**

Across the included studies, surface topography of polymeric biomaterials consistently influenced osteoblast adhesion. It depended upon Feature size (nano vs micro), Geometry (pits, grooves, pillars, pores, fibres), Surface roughness and Degree of order (ordered vs disordered). With regard to the effect of Nanotopography (10–200 nm range), it showed the Strongest and most consistent enhancement of adhesion. Disordered nanotopographies increased focal adhesion formation, cytoskeletal organisation, and mechanotransduction. Nanopits increased adhesion but sometimes reduced large focal adhesion complexes. Nanogratings at 30 nm caused alignment and organised adhesion. Etched nanorough surfaces elevated the osteoblast adhesion. Summarily, Nanotopography regulates cell–substrate signalling through FAK and integrins, rather than just physical anchorage. On the other hand,

Microtopography (1–100 μm range) had a strong influence on cell morphology and alignment, as Micropatterns showed
"Cell-instructive" behaviour and Contact guidance. Smaller pores (0.2–1 μm) caused better spreading, and larger pores led to rounded morphology. While naotopography enhanced adhesion, microtopography had a role in cell organisation, orientation, and cytoskeletal arrangement, which is an indirect pathway to influencing adhesion. Hierarchical or Combined Micro–Nano Topography mimics natural bone ECM, which is optimal for multi-scale mechanotransduction.
With regard to surface roughness, moderate roughness showed optimal adhesion, while smooth surfaces showed poor adhesion. Also, an excessively rough surface reduces cell spreading. Therefore, an optimal roughness window is apparent and rules out a linear relationship. Geometry of the surface, such as pits, grooves, gratings, and spherulites, dictates the cell shape and consequent adhesion strength. With regard to cell types, primary osteoblasts are more sensitive to nanotopography, but Cell lines are more robust but are still responsive. This may be a limitation in result consolidation due to cell model heterogeneity. The role of fabrication method also influences surface chemistry, and energy also influences adhesion. Most frequently used technique of assessing adhesion was Imaging (fluorescence / SEM), followed by Cell counting assays and MTT / viability assays, inferring adhesion indirectly. Most included studies were found to have a moderate risk of bias, due to incomplete reporting of quantitative adhesion assays in addition to limited statistical treatment. Studies reporting advanced nanomodification techniques exhibited low RoB.

Discussion

The current systematic review has evaluated polymeric biomaterials used for bone implantation and has assessed the role of their surface topography in osteoblast adhesion. It has been seen that there is strong Evidence to show that nanotopography significantly enhances the osteoblast adhesion. Also, surface roughness positively correlates with adhesion, although not related linearly. Microtopography is seen to direct the cell alignment and morphology, thereby indirectly affecting the adhesion. However, lack of standardisation in adhesion assays and heterogeneous reporting of roughness parameters and feature size quantification have limited the applications of the findings.

From the viewpoint of mechanisms by which the topography influences cell adhesion, the primary mechanism broadly pointed out in the included papers is the integrin-mediated attachment leading to Focal adhesion complex formation. Another mechanism is the role of Cytoskeletal organisation (actin, myosin) through the mechanotransduction pathways (FAK signalling). Both these are heavily interrelated pathways, but are differently influenced by the materials. This may be the reason for microtopography influencing shape and nanotopography affecting adhesion. Topography signals the integrin clustering and ligand binding, while nanoscale features may promote focal adhesion complex formation. Disordered nanotopography leads to stronger cytoskeletal tension, all of which leads to downstream osteogenic differentiation signals.(37,38)

Cell lines used in the included studies were primary osteoblasts of various origins and cell lines such as SaOS2 and MG63. Minor changes may be due to differences in response due to differences in the physiology of primary cells and cell lines. Predominant methodology used to assess adhesion was imaging by various modalities such as SEM, fluorescent staining, etc. These are fine techniques to visualise cell morphology, but nevertheless are not completely quantitative, such as MTT or alamar blue assays. Hence, articles included in this study have analysed the adhesion based on shape and localisation effectively, but have not quantified the number biochemically. This may be seen as a limitation in the literature.

For the Nanotopography, the optimal range has been found to be 10–100 nm, which promotes Cell spreading, Lamellipodia formation and Stable adhesion. Also, it must be emphasised that geometry dictates cytoskeletal architecture, which in turn governs the adhesion.

Surface roughness has been easily produced by various techniques, such as etching in polymers. The outcome is an irregularly formed surface. These are characterised by various techniques such as AFM or STM, and the roughness has been found to relate to the adhesion of cells. Multiple studies in this review have shown that increasing roughness increases cell attachment. Studies such as Han et al. (2022) (PCL)(19), Wang et al. (2000) (polyesterurethane)(33), Smith et al. (2007)(PLGA)(30), Filipov et al. (2022)(PCL)(18) have supported this view. However, studies including Melčová et al. (2024) (PHB/PLA), Lee et al. (2004)(Polycarbonate)(21), Sun et al. (2010)(Polystyrene)(31), and Lim et al. (2005)(PLLA)(24) have reported improved spreading on smaller micropores compared to larger ones. It has been seen in this systematic review that while a clear relation exists between roughness and cell adhesion, there appears to be an optimal range for the best adhesion of osteoblast cells, below or above which the cell adhesion appears to fall below the optimum level. At the optimum roughness level, there is increased protein adsorption and integrin binding, leading to increased adhesion. On the other hand, excessive roughness reduced cell spreading and viability. Table 3 summarises the broader picture of the findings seen in this systematic review.

Table. 3. Summary of Topography vs Osteoblast adhesion

Topography Category	Subtype / Geometry	Feature Size Range	Adhesion Outcome	Mechanistic Interpretation
Nanotopography	Disordered nanopits / nanoislands	10–100 nm	increase Adhesion, focal adhesions, and cytoskeletal organization	Promotes integrin clustering and focal adhesion maturation; enhances mechanotransduction

Topography Category	Subtype / Geometry	Feature Size Range	Adhesion Outcome	Mechanistic Interpretation
	Ordered nanopits / nanopores	~100–200 nm	Mixed: decrease large adhesion complexes but increase osteogenic signaling	Restricts focal adhesion size but enhances signaling pathways (FAK-mediated)
	Nanogratings	<30 nm vs >30 nm height	Threshold-dependent: alignment and adhesion increase at >30 nm	Topography-guided cytoskeletal alignment and anisotropic force distribution
	Nanorough surfaces (etched)	~50–100 nm	increased Adhesion	Increased surface energy and protein adsorption enhances cell attachment
Microtopography	Micropatterns (engineered shapes)	0.5–15 μm	Geometry-dependent adhesion; increased spreading	"Cell-instructive" behavior via spatial control of adhesion sites
	Microgrooves	50–500 nm depth, periodic	increased Alignment, and directional adhesion	Contact guidance via cytoskeletal reorganization
	Micropores	0.2–8 μm	Smaller pores increase adhesion; larger pores decrease spreading	Optimal pore size supports focal adhesion anchoring
Hierarchical (Micro + Nano)	Combined micro/nano pits or roughness	nm–μm combined	increased adhesion and proliferation	Mimics extracellular matrix architecture → multi-scale signaling
Porous Topography	Microporous / scaffold porosity	μm–mm scale	increased adhesion (optimal porosity dependent)	Enhances surface area and nutrient diffusion; supports anchorage
Laser-	Micro/nano	μm scale +	increased	Combined roughness +

Topography Category	Subtype / Geometry	Feature Size Range	Adhesion Outcome	Mechanistic Interpretation
textured Surfaces	roughness patterns	nano roughness	Adhesion	chemistry modification improves cell interaction
Crystallization-Induced Topography	Spherulites / banded morphology	35–350 nm	increased Adhesion; spatial localization in valleys	Topography provides contact guidance and preferential adhesion zones
Phase-Separated (Demixed) Topography	Nano-islands / domains	3–100 nm	increase adhesion (optimal at ~10–20 nm)	Height-dependent lamellipodia formation and spreading
Gradient Topography	Gradient nanogratings	0–350 nm height	Adhesion/orientation varies with height	Cells sense nanoscale gradients and adapt adhesion dynamically
Roughness-Dominated Surfaces	Random roughness	nm–μm	Moderate roughness increases adhesion; excessive roughness decreases cell number	Optimal roughness enhances integrin binding; excessive disrupts spreading

Further, Disordered nanotopography is more biomimetic and enhances adhesion and differentiation, while ordered structures may offer reproducibility and precise control over cell alignment. Fabrication technique may leave its signature of surface energy and wettability, leading to its influence on cell adhesion. This review has critically analysed the role of surface topography in cell adhesion. With the current trend of rising polymeric bone implants, this paper throws valuable light on designing optimally prepared surfaces. Nanotopography (~10–100 nm) with moderate microscale roughness (0.1 to 10 microns) may be the recommended topography for cell adhesion, based on studies included.

With regard to limitations of this review, it should be noted that Roughness parameters vary among the studies, where Ra, Sa, and Rq were not interchangeable across them. Several studies report feature size instead of true roughness, and also, surface chemistry and wettability may act as confounders. The RoB analysis showed low to moderate bias, facilitating application of the findings without limitation from bias.

Conclusions

This systematic review found that surface topography played a major role in bone cell adhesion. Next, disordered nanotopography was found to be more biomimetic and enhanced

adhesion and differentiation, while ordered structures may offer reproducibility with precise control over cell alignment. Nanotopography (~10–100 nm) with moderate microscale roughness (0.1 to 10 microns) may be the recommended topography for cell adhesion, based on studies included. Finally, fabrication techniques may leave their signature of surface energy and wettability, leading to their influence on cell adhesion.

References

1. Feller L, Jadwat Y, Khammissa RA, Meyerov R, Schechter I, Lemmer J. Cellular responses evoked by different surface characteristics of intraosseous titanium implants. Biomed Res Int. 2015;2015:171945. doi: 10.1155/2015/171945.
2. Albrektsson T, Wennerberg A. On osseointegration in relation to implant surfaces. Clin Implant Dent Relat Res. 2019 Mar;21 Suppl 1:4-7. doi: 10.1111/cid.12742.
3. Tuikampee S, Chaijareenont P, Rungsiyakull P, Yavirach A. Titanium surface modification techniques to enhance osteoblasts and bone formation for dental implants: a narrative review on current advances. Metals. 2024 Apr 28;14(5):515. doi: 10.3390/met14050515
4. Orapiriyakul W, Young PS, Damiati L, Tsimbouri PM. Antibacterial surface modification of titanium implants in orthopaedics. J Tissue Eng. 2018 Jul 25;9:2041731418789838. doi: 10.1177/2041731418789838.
5. Kuhn S, Kroth J, Ritz U, Hofmann A, Brendel C, Müller LP, Förch R, Rommens PM. Reduced fibroblast adhesion and proliferation on plasma-modified titanium surfaces. J Mater Sci Mater Med. 2014 Nov;25(11):2549-60. doi: 10.1007/s10856-014-5278-1.
6. Prasad A. State of art review on bioabsorbable polymeric scaffolds for bone tissue engineering. Materials Today: Proceedings. 2021 Jan 1;44:1391-400. doi: 10.1016/j.matpr.2020.11.622
7. Kalirajan C, Dukle A, Nathanael AJ, Oh TH, Manivasagam G. A Critical Review on Polymeric Biomaterials for Biomedical Applications. Polymers (Basel). 2021 Sep 6;13(17):3015. doi: 10.3390/polym13173015.
8. Zhou K, Wang M, Zhang S, Huo J, Zheng W, Abueida MR, Wang Q, Liu H, Yi Z. Titanium alloys for orthopedic applications: A review on the osteointegration induced by physicomechanical stimuli. Journal of Materials Research and Technology. 2024 May 1;30:8260-76. doi: 10.1016/j.jmrt.2024.05.207
9. Haddaway, N. R., Page, M. J., Pritchard, C. C., & McGuinness, L. A. (2022). PRISMA2020: An R package and Shiny app for producing PRISMA 2020-compliant flow diagrams, with interactivity for optimised digital transparency and Open Synthesis Campbell Systematic Reviews, 18, e1230. https://doi.org/10.1002/cl2.1230
10. Ajami-Henriquez D, Rodríguez M, Sabino M, Castillo RV, Müller AJ, Boschetti-de-Fierro A, Abetz C, Abetz V, Dubois P. Evaluation of cell affinity on poly(L-lactide) and poly(epsilon-caprolactone) blends and on PLLA-b-PCL diblock copolymer surfaces.J Biomed Mater Res A. 2008 Nov;87(2):405-17. doi: 10.1002/jbm.a.31796.
11. Allan, C.; Ker, A.; Smith, C.-A.; Tsimbouri, P.M.; Borsoi, J.; O'Neill, S.; Gadegaard, N.; Dalby, M.J.; Meek, R.M.D. Osteoblast response to disordered nanotopography.Journal of Tissue Engineering 2018;9 pp-. doi: 10.1177/2041731418784098

12. Barata D, Dias P, Wieringa P, van Blitterswijk C, Habibovic P. Cell-instructive high-resolution micropatterned polylactic acid surfaces.Biofabrication. 2017 Jul 24;9(3):035004. doi: 10.1088/1758-5090/aa7d24.
13. Biggs MJ, Richards RG, Gadegaard N, McMurray RJ, Affrossman S, Wilkinson CD, Oreffo RO, Dalby MJ. Interactions with nanoscale topography: adhesion quantification and signal transduction in cells of osteogenic and multipotent lineage.J Biomed Mater Res A. 2009 Oct;91(1):195-208. doi: 10.1002/jbm.a.32196.
14. Cha KJ, Hong JM, Cho DW, Kim DS. Enhanced osteogenic fate and function of MC3T3-E1 cells on nanoengineered polystyrene surfaces with nanopillar and nanopore arrays.Biofabrication. 2013 Jun;5(2):025007. doi: 10.1088/1758-5082/5/2/025007.
15. Dalby MJ, McCloy D, Robertson M, Agheli H, Sutherland D, Affrossman S, Oreffo RO. Osteoprogenitor response to semi-ordered and random nanotopographies.Biomaterials. 2006 May;27(15):2980-7. doi: 10.1016/j.biomaterials.2006.01.010.
16. DeSantis PM, Barnes E, Derr T, Spece H, Kurtz SM. Porous Additively Manufactured PEKK Improves In Vitro Osteoblastic Performance Compared to PEEK.J Orthop Res. 2026;44(2026): e70069. doi: 10.1002/jor.70069.
17. Duan S, Yang X, Mao J, Qi B, Cai Q, Shen H, Yang F, Deng X, Wang S. Osteocompatibility evaluation of poly(glycine ethyl ester-co-alanine ethyl ester)phosphazene with honeycomb-patterned surface topography.J Biomed Mater Res A. 2013 Feb;101(2):307-17. doi: 10.1002/jbm.a.34282.
18. Filipov E, Angelova L, Vig S, Fernandes MH, Moreau G, Lasgorceix M, Buchvarov I, Daskalova A. Investigating Potential Effects of Ultra-Short Laser-Textured Porous Poly-ε-Caprolactone Scaffolds on Bacterial Adhesion and Bone Cell Metabolism.Polymers (Basel). 2022 Jun 12;14(12):2382. doi: 10.3390/polym14122382.
19. Han J, Li Z, Sun Y, Cheng F, Zhu L, Zhang Y, Zhang Z, Wu J, Wang J. Surface Roughness and Biocompatibility of Polycaprolactone Bone Scaffolds: An Energy-Density-Guided Parameter Optimization for Selective Laser Sintering.Front Bioeng Biotechnol. 2022 Jul 11;10:888267. doi: 10.3389/fbioe.2022.888267.
20. Kryszak, B.; Szustakiewicz, K.; Dzienny, P.; Junka, A.; Paleczny, J.; Szymczyk-Ziółkowska, P.; Hoppe, V.; Antończak, A. Functionalization of the PLLA surface with a femtosecond laser: Tailored substrate properties for cellular response.Polymer Testing 2022;116() 107815pp-. doi: 10.1016/j.polymertesting.2022.107815
21. Lee, S.J.; Choi, J.S.; Park, K.S.; Khang, G.; Lee, Y.M.; Lee, H.B. Response of MG63 osteoblast-like cells onto polycarbonate membrane surfaces with different micropore sizes.Biomaterials 2004;25(19) pp: 4699-4707. doi: 10.1016/j.biomaterials.2003.11.034
22. Lenhert, S.; Meier, M.-B.; Meyer, U.; Chi, L.; Wiesmann, H.P. Osteoblast alignment, elongation and migration on grooved polystyrene surfaces patterned by Langmuir-Blodgett lithography.Biomaterials 2005;26(5) pp563-570doi: 10.1016/j.biomaterials.2004.02.068
23. Li W, Lu L, Jiao Y, Zhang C, Zhou C. Poly(L-lactide) crystallization topography directs MC3T3-E1 cells response.J Biomater Sci Polym Ed. 2016 Sep;27(13):1317-30. doi: 10.1080/09205063.2016.1196530.
24. Lim JY, Hansen JC, Siedlecki CA, Hengstebeck RW, Cheng J, Winograd N, Donahue HJ. Osteoblast adhesion on poly(L-lactic acid)/polystyrene demixed thin film blends: effect of

nanotopography, surface chemistry, and wettability.Biomacromolecules. 2005 Nov-Dec;6(6):3319-27. doi: 10.1021/bm0503423.
25. Lim JY, Hansen JC, Siedlecki CA, Runt J, Donahue HJ. Human foetal osteoblastic cell response to polymer-demixed nanotopographic interfaces.J R Soc Interface. 2005 Mar 22;2(2):97-108. doi: 10.1098/rsif.2004.0019.doi:10.1098/rsif.2004.0019
26. Lin, S.; Yuan, X.; Du, X.; An, R.; Han, Y. Surface microtopography construction and osteogenic properties evaluation of bulk polylactic acid implants.Colloids and Surfaces B: Biointerfaces 2023;228() 113418pp-doi: 10.1016/j.colsurfb.2023.113418
27. Maclaine SE, Gadhari N, Pugin R, Meek RM, Liley M, Dalby MJ. Optimizing the osteogenicity of nanotopography using block co-polymer phase separation fabrication techniques.J Orthop Res. 2012 Aug;30(8):1190-7. doi: 10.1002/jor.22076.
28. Melčová, V.; Krobot, Š.; Šindelář, J.; Šebová, E.; Rampichová, M.K.; Přikryl, R. The effect of surface roughness and wettability on the adhesion and proliferation of Saos-2 cells seeded on 3D printed poly(3-hydroxybutyrate)/polylactide (PHB/PLA) surfaces.Results in Surfaces and Interfaces 2024;16:100271 pp-. doi: 10.1016/j.rsurfi.2024.100271
29. Riehle, M.O.; Dalby, M.J.; Johnstone, H.; Macintosh, A.; Affrossman, S. Cell behaviour of rat calvaria bone cells on surfaces with random nanometric features.Materials Science and Engineering C 2003;23(3) pp337-340. doi: 10.1016/S0928-4931(02)00282-5
30. Smith LL, Niziolek PJ, Haberstroh KM, Nauman EA, Webster TJ. Decreased fibroblast and increased osteoblast adhesion on nanostructured NaOH-etched PLGA scaffolds. Int J Nanomedicine. 2007;2(3):383-8. PMID: 18019837; PMCID: PMC2676656.
31. Sun J, Ding Y, Lin NJ, Zhou J, Ro H, Soles CL, Cicerone MT, Lin-Gibson S. Exploring cellular contact guidance using gradient nanogratings.Biomacromolecules. 2010 Nov 8;11(11):3067-72. doi: 10.1021/bm100883m.
32. Wan Y, Wang Y, Liu Z, Qu X, Han B, Bei J, Wang S. Adhesion and proliferation of OCT-1 osteoblast-like cells on micro- and nano-scale topography structured poly(L-lactide).Biomaterials. 2005 Jul;26(21):4453-9. doi: 10.1016/j.biomaterials.2004.11.016.
33. Wang JH, Yao CH, Chuang WY, Young TH. Development of biodegradable polyesterurethane membranes with different surface morphologies for the culture of osteoblasts. J Biomed Mater Res. 2000 Sep 15;51(4):761-70. doi: 10.1002/1097-4636(20000915)51:4<761::aid-jbm26>3.0.co;2-2. PMID: 10880126.
34. Wang, K.; Jesse, S.; Wang, S. Banded spherulitic morphology in blends of poly (propylene fumarate) and poly(ε-caprolactone) and interaction with MC3T3-E1 cells.Macromolecular Chemistry and Physics 2012;213(12) pp1239-1250. doi: 10.1002/macp.201200004
35. Yeon, S.-J.; Lee, J.W.; Lee, J.-W.; Jeong, E.J.; Kwark, Y.-J.; Kim, S.H.; Lee, K.Y. Responses of preosteoblasts on nano-structured polymer surfaces prepared from block copolymer-surfactant complexes.Soft Matter 2012;8(30) pp7898-7903 doi: 10.1039/c2sm25222h
36. Yuanzheng W, Qilin J, Xin H, Shaohong W, Jinlong L, Jian C, Zhongxing L. Enhancing bone repair ability of 3D-printed PLLA scaffolds via N-methyl-2-pyrrolidone etching.J Mater Sci Mater Med. 2026 Jan 28;37(1):32. doi: 10.1007/s10856-026-07005-6.

37. Frey MT, Tsai IY, Russell TP, Hanks SK, Wang YL. Cellular responses to substrate topography: role of myosin II and focal adhesion kinase. Biophys J. 2006 May 15;90(10):3774-82. doi: 10.1529/biophysj.105.074526.
38. Cavalcanti-Adam EA, Aydin D, Hirschfeld-Warneken VC, Spatz JP. Cell adhesion and response to synthetic nanopatterned environments by steering receptor clustering and spatial location. HFSP J. 2008 Oct;2(5):276-85. doi: 10.2976/1.2976662.